Green Chemistry

PAPER

View Article Online
View Journal | View Issue

Cite this: *Green Chem.*, 2022, **24**, 3834

Chitin nanowhiskers with improved properties obtained using natural deep eutectic solvent and mild mechanical processing†

Huy Vu Duc Nguyen, [a] Renko de Vries [a] and Simeon D. Stoyanov *[a,b,c]

Traditionally, chitin nanowhiskers (ChNW) have been synthesized using acid or alkali hydrolysis, which is not a fully green and sustainable process. Here, we demonstrate a novel, two-step, environmentally friendly process for producing chitin nanowhiskers with improved yield and colloidal stability. The process begins by swelling the amorphous regions of native chitin in a Natural Deep Eutectics Solvent (NADES). It is followed by a mild mechanical treatment (defibrillation) by injecting chitin-NADES suspension into rotor-stator colloidal mill filled with water, which is aimed to separate crystalline domains of the native chitin into individual nanowhiskers. This approach produces ChNW suspensions with higher yield and improved colloidal stability when compared to the conventional method of producing ChNW using acid hydrolysis. We hypothesized that this is due to the residual amorphous chitin that remains attached to the surface of the nanocrystalline whiskers, which provides additional steric stability to the ChNW suspensions. Furthermore, we find that ChNW produced by our method has better compatibility with secondary polymer matrices such as polyvinyl alcohol (PVOH), resulting in nanocomposite polymer films with better mechanical performance.

Received 23rd January 2022,
Accepted 5th April 2022

DOI: 10.1039/d2gc00305h

rsc.li/greenchem

1. Introduction

The increased awareness of climate change and other environmental issues has led to a strong interest in developing more sustainable polymeric materials from natural sources and using environmentally friendly solvents and fabrication processes.[1] An attractive alternative in this respect is the direct use of abundantly available biopolymers. For example, the polysaccharide chitin is the second or third most abundant natural biopolymer on Earth, after cellulose and possibly lignin. It is the primary structural polymer of many crustaceans and insects' exoskeletons and cell walls of fungi.

Chitin is well-known for its low toxicity, biocompatibility, and biodegradability. Given its abundance, it has the potential to become an important polymer ingredient in a future bio-based materials economy. Indeed, chitin has already been explored and used in pharmaceutical, biomedical,[2] packaging, and food applications,[3] as well as adsorbent.[4]

Although chitin has a wide range of possible applications, its usage in applications is still limited due to the diversity of chitin's sources and the technique by which it is extracted.[5] Generally, chitin is isolated primarily from crustacean biomass and undergoes a series of chemical processes such as decolorization, deproteination, demineralization to obtain the purified chitin materials, dramatically affecting the physicochemical properties of chitin material.[6] Even with the use of purified chitin, a significant challenge for the direct use to produce new chitin materials is the limited number of available solvents that are sufficiently sustainable. Like chemically related compound, cellulose, the tightly packed crystalline structures, and intensive intra- and intermolecular hydrogen bodings (H-bonds) network give chitin a very stable structure that is insoluble in most solvents. As a result, chitin is soluble in very few solvents, considered non-green, non-sustainable, or expensive, and might require very special processing conditions with high energy demand. Examples are *N*,*N*-dimethylacetamide (DMAc)/lithium chloride (LiCl), aqueous NaOH/urea, very strong acids, and fluorinated solvents.[7] Several studies have also been performed using ionic liquid (ILs) to dissolve chitin raw materials. For example, the room-temperature ionic liquid (RTIL), 1-butyl-3-methylimidazolium acetate ([Bmim][Ac]), is proposed as a suitable solvent for native chitins with different

[a]*Laboratory of Physical Chemistry and Soft Matter, Agrotechnology & Food Sciences Group, Wageningen UR, Wageningen 6708WE, The Netherlands. E-mail: simeon.stoyanov@wur.nl*
[b]*Department of Chemical and Biomolecular Engineering, North Carolina State University, Raleigh, North Carolina 27695, USA*
[c]*Department of Mechanical Engineering, University College London, Torrington Place, London WC1E 7JE, UK*

† Electronic supplementary information (ESI) available. See DOI: https://doi.org/10.1039/d2gc00305h

sources and molecular weight.[8] Another study suggested that an IL, 1-ethyl-3-methyl-imidazolium acetate, can be used for the complete extraction of chitin from raw crustacean shells, leading to a high purity high molecular weight chitin powder.[9] However, the use of ILs and similar solvents for large-scale industrial applications is still problematic given their costs and concerns about their recycling and environmental sustainability.

Chitin from natural sources is typically semi-crystalline, consisting of chitin nanocrystals embedded in a matrix of amorphous chitin. When isolated from chitin-containing materials, these chitin nanocrystals often have rod-like morphologies 10–20 nm in width and approximately 200–300 nm in length, referred to as chitin nanowhiskers (ChNW). These nanomaterials have been proposed as functional ingredients for various applications such as to create mesoporous aerogels,[10] to enhance the perception of salt in foods,[11] to stabilize foams,[12] and as a sustainable reinforcing agent for nanocomposite polymer films.[13–15]

The most widely used approach for obtaining ChNW from semi-crystalline chitin materials is still acid hydrolysis.[7] Disadvantages of this method are the significant loss of material,[16,17] large volumes of acidic wastewater, and partial deacetylation of the chitin, which may not always be desirable. Other methods for producing ChNW from raw materials were also developed using 2,2,6,6-tetramethylpiperidine-1-oxyl (TEMPO) oxidation and high-energy mechanical defibrillation with high-pressure homogenizers and microfluidizers.[18,19] Both have their own advantages and disadvantages. For example, TEMPO oxidation is only specific to β-chitin derived from squid pen.[19] Additionally, the process introduces carboxylic acid or carboxylate groups that may not always be desired. In the literature, mechanical treatment alone has also been reported as a method for obtaining ChNW and chitin nanofibers using grinding[20] or mechanical defibrillation.[21]

Deep Eutectic Solvents (DES) are mixtures of two or more components associated with each other through strong hydrogen bonding, having much lower melting temperatures than individual components.[22] DES, composed of small molecules derived from nature, are called Natural Deep Eutectic Solvents (NADES). Given that the solubility problems with chitin and cellulose are linked to their ability to form extensive intra- and inter-hydrogen bond networks, it is a reasonable assumption that a specific DES or NADES, which likewise is formed through H-bond formation, could act as a (partial) solvent for these materials *via* H-bond interaction. In light of this hypothesis, the application of DES to produce cellulose nanocrystals (CNCs) was first introduced and explored by Sirvio *et al.*[23] In this study, authors reported the use of several DESs obtained from choline chloride and different organic acids to fabricate CNCs from dissolving pulp. The studied DESs showed efficiency in pre-treating wood fiber into microsized fibers, and CNCs were individualized using a microfluidizer. However, high-pressure homogenizers or microfluidizers consume much energy and are not cost-effective processing methods. After this pioneering study, there have been several other studies conducted to prepare CNCs using DES in combining with ultrasonic or mechanical treatment to facilitate the production conditions.[24,25]

Correspondingly, the use of DES to produce chitin nanofiber and nanowhiskers has been reported from several previous studies. For example, Mukesh *et al.* reported the production of chitin nanofibers using a deep eutectic solvent (choline chloride–thiourea) and applied the nanofibers as reinforcement fillers for calcium alginate.[26] Yuan *et al.* reported using different acidic-based DES combined with ultrasonic treatment to prepare ChNW from crab shells.[27] In another study from the same group, Hong *et al.* proposed that a different eutectic solvent derived from ferric chloride hexahydrate and betaine chloride can also be used as sufficient media to produce ChNW.[28] Generally speaking, while previous studies have mainly focused on optimizing (NA)DES-based extraction of ChNW from raw materials without explicitly considering mechanical processing as a key variable in any detail.[27,28] Here, we not only systematically combine NADES pre-treatments with controlled and mild mechanical processing (defibrillation) for ChNW extraction, we also investigate in detail how the physical properties of the NADES-ChNW that we obtain differ from those obtained by traditional acid hydrolysis (Ac-ChNW).

Previously, in the context of cellulose regeneration, we have thoroughly characterized the NADES composed of Choline chloride and Malic acid (CM).[29] It has already been reported that CM effectively extracts ChNW from powdered shrimp shells.[27] Here, we take CM as a model NADES and combine it with mild mechanical processing to obtain NADES-ChNW. The physical properties of the NADES-ChNW are compared to those of Ac-ChNW obtained by traditional acid hydrolysis.

As representative physical properties, we focus on the colloidal stability and rheology of ChNW dispersions (high water activity case) and the compatibility with polymers such as polyvinyl alcohol (PVOH) when being used as fillers in nanocomposite films (low water activity case).

The fundamental physical properties of ChNW that we investigate are primarily determined by the interactions of the ChNW with each other (in suspensions) or with other polymers (when used as fillers in nanocomposite polymer films). In turn, these interactions are mainly determined by the surface structure and chemistry of the ChNW.

Our hypothesis, represented in Fig. 1, is that the combined approach using NADES treatment and mild mechanical processing does not remove the bulk of the amorphous chitin polymers present in the original chitin material. In contrast, acid hydrolysis does essentially remove this material. Therefore, we speculate this amorphous chitin must be left as a thin (brush) layer on the surface of the NADES-ChNW, making their surface chemistry substantially different from that of Ac-ChNW. Specifically, we attribute the higher dispersion stability and better compatibility with polymers such as PVOH in nanocomposite films to the presence of this amorphous chitin layer on the outside of the NADES-ChNW.

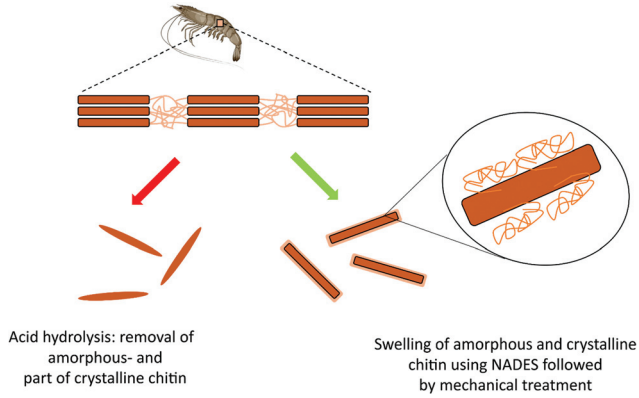

Fig. 1 Hypothesis outlines the main difference between ChNW obtained by acid hydrolysis (Ac-ChNW) and ChNW obtained by NADES pre-treatment followed by mild mechanical processing (NADES-ChNW).

2. Experimental

2.1 Materials

High purity grade choline chloride (CC) and D-L-malic acid (MA) were purchased from VWR Life Science. Chitin powder (from shrimp shells, practical grade) was obtained from Sigma Aldrich (Lot# SLCC6812) and was used without further purification. Poly(vinyl alcohol) (PVOH), M_w: 89 000–98 000; 99% hydrolyzed was obtained from Sigma Aldrich.

2.2 Preparation of chitin nanowhiskers

The NADES solvent, composed of choline chloride (CC) and malic acid (MA), was prepared following previously reported protocols.[29] We chose to use a 1.5 : 1 CC : MA molar ratio to prepare chitin nanowhiskers in this study as it was giving the most optically clear and homogeneous chitin dispersions. Chitin powder was used directly without any further purification or treatment. Different amounts of chitin (from 1 wt% to 7 wt% to the weight of CM NADES) were added into the beaker with 10 grams of CM NADES under magnetic stirring. The mixture was then followed by an overnight temperature-controlled swelling/dissolution step in an oil bath at 80 °C. The obtained mixture we refer to as a complete swelling mixture can be recognized by the homogenous dispersions having honey-like viscosity and amber-like color. The resulting mixtures were then transferred into 10 ml syringes and gradually injected into the entrance of the lab-scale rotor-stator colloidal mill (IKA Magic Lab), prefilled with ambient temperature, Milli-Q water, and operated at 15 000 rpm (gap size = 0.159 mm). For 30 minutes, the output stream was recirculated while the chitin-NADES solution/dispersion was gradually injected. The idea of this process is two fold: first, to change the solvent quality and possibly precipitate any low molecular weight (LMW) chitin that might be solubilized or dissolved in NADES, and most importantly, to disrupt the amorphous domains and liberate (defibrillate) the individual chitin nanocrystals. The obtained chitin nanowhiskers suspension was further diluted with Milli-Q water and then centrifuged at 13 000 rpm for 10 min. This step was repeated 5 times to remove all the NADES solvent and LMW chitin. Then, to further remove the residual solvents and any LMW residues, the suspension has been dialyzed using a cellulose dialysis membrane with a cut-off limit of 3.5 kDa. Finally, we adjusted samples' pH to around 6 and kept them in these conditions for further experiments or freeze-dried to obtain powder form for long-term storage and further experiments.

To compare with the chitin nanowhiskers prepared by our approach, namely: NADES-ChNW, the ChNW by acid hydrolysis: Ac-ChNW were obtained following the literature's method[30] but without purification step used in this work. And after that the obtained Ac-ChNW suspensions were treated in the same way as the NADES-ChNW.

2.3 Characterization of chitin nanowhiskers

Transmission electron microscope (TEM). ChNW samples were prepared by depositing 5 μL of 0.01% ChNW suspensions onto glow-discharged carbon-coated CF400-CU TEM grids (Electron Microscopy Sciences, USA). Excess liquid was blotted away with filter paper. The specimens were then negatively stained for 20 s using a 2% aqueous uranyl acetate solution; the excess staining solution was blotted to remove by a filter paper, then samples were allowed to dry under the ambient condition. The samples were observed using a JEM-1400Plus transmission electron microscope, using 100 kV accelerating voltage, and a JEOL Ruby CCD camera. The average values of width and length of chitin nanowhiskers were analyzed and calculated using Image J. The dimensions of the chitin nanowhiskers were averaged based on 150 representative items.

Scanning electron microscope (SEM). Scanning electron microscopy (SEM) was performed to investigate the morphology of fresh ChNW and freeze-dried NADES-ChNW samples. Suspension of fresh ChNW was first spin-coated onto a silica substrate. Subsequently, these fresh ChNW and freeze-dried samples were mounted on SEM stubs by carbon adhesive tabs and sputter-coated with 12 nm Tungsten (Leica MED 020, Switzerland). Samples were analyzed at 2 kV, 6 pA, in a Field Emission Scanning Electron Microscope (Magellan 400, FEI, the Netherlands).

Fourier transform infrared. Fourier transform infrared (FT-IR) measurements of native chitin powder and freeze-dried ChNW powder were carried out using a Bruker FT-IR equipped with OPUS software and an ATR sampling accessory. Spectra were acquired for wavenumber from 400 to 4000 cm^{-1} with a resolution of 4 cm^{-1} in transmittance mode. Each spectrum was the average of 32 scans.

Solid-state ^{13}C NMR. Solid-state ^{13}C NMR spectra were acquired on a Bruker Avance AV700 U spectrometer, samples with 25–30 mg of native chitin powder and freeze-dried regenerated chitin were packed into 3.2 mm magic-angle spinning (MAS) rotors. The relaxation delay (5 s), acquisition time (50 ms), and contact time (1 ms) were used. A total of 2048 scans were acquired for each spectrum.

X-ray diffraction (XRD). XRD spectra were collected on a Bruker D8 ADVANCE XRD diffractometer using a Cu Kα radi-

ation source (λ = 0.15418 nm) at a voltage of 40 kV and a current of 40 mA. For the powder characterization, native chitin powder and freeze-dried samples were pressed between two glass slides into 1 mm thick flat sheets. XRD patterns were recorded from 5 to 60° (2θ) at room temperature with a step size of 0.02° and a scan time of 38 s per step.

The crystallinity indices (CrI) of native and freeze-dried ChNW samples were calculated after removing the background intensity:

$$\mathrm{CrI} = \frac{I_o - I_{am}}{I_o} \times 100\,(\%) \quad (1)$$

where I_o is the height of the (110) peak, and I_{am} is the height of amorphous scattering at $2\theta = 16°$.[31]

The mixtures of chitin-NADES were measured on the same diffractometer, equipped with a TTK 600 cooling chamber (Anton Paar). The samples were cooled from the room temperature to −90 °C using liquid nitrogen. These measurements were operated at −90 °C and recorded at the same working conditions as the powder measurements.

Conductometric titration. The amino group content of the fresh NADES-ChNW and Ac-ChNW suspensions was determined by conductometric titration. First, 100 ml of 0.1 wt% aqueous suspensions of each ChNW sample was treated with 1 ml HCl 1 M to fully protonate the amino group on the surface of chitin nanowhiskers. Conductometric titration was performed by adding 0.01 M sodium hydroxide (NaOH) under gentle stirring (100 rpm). Conductivity and pH values of the ChNW suspension were simultaneously monitored using a pH meter and a conductivity meter.[32]

2.4 Stability of Chitin nanowhiskers (ChNW) colloidal system

Dynamic and electrophoretic light scattering. The ChNW suspension was prepared by diluting the samples to 0.1 wt%. The measurements were performed using a Zetasizer NanoSeries instrument (Malvern Instruments Ltd, U.K.) equipped with a He–Ne laser (633 nm) at a scattering angle of 173° at room temperature T = 20 °C. The average hydrodynamic particle sizes were reported using the Zetasizer software version 7.13 (Malvern, UK). For the pH-dependent measurements, the pH value of ChNW suspension was adjusted in the pH range from 2 to 12 pH by adding either 0.1 N HCl or 0.1 N NaOH. Hydrodynamic sizes and zeta potential were measured over this range of pH values. For the ionic strength-dependent measurement, pH values of all suspensions were kept at 4. Three replicates were done for each sample.

Rheological behavior of ChNW suspensions. The resulting NADES-ChNW suspensions were freeze-dried to obtain powder form. Freeze-dried NADES-ChNW powder was redispersed into Milli-Q water with different amounts by weight to make various ChNW suspensions. Then, the rheological behavior of these ChNW suspensions was measured using an MCR 501 Rheometer (Anton Paar, Austria) equipped with cone-plate geometry (4°–25 mm) and a Peltier temperature control system. The viscosity of the aqueous chitin nanowhiskers suspensions was tested over a shear rate range of 0.01 to 500 s^{-1}. A frequency sweep to study the viscoelasticity was performed at an oscillatory strain of 1%, determined to be within the linear viscoelastic regime according to oscillatory strain sweeps. Time-dependent behavior of redispersed NADES-ChNW suspensions was investigated at different shear-rate conditions: at 0.1 s^{-1}, 100s^{-1}, and 0.1 s^{-1}, respectively.

Preparation and characterization of ChNW polymer composites. A 6 wt% polyvinyl alcohol (PVOH) solution was prepared by dissolving an exact quantity of PVOH in warm water for 2 h. Various PVOH-ChNW nanocomposite compositions with different concentrations by weight of ChNW (2, 4, 6, 8, 10 wt%) compared to the amount of PVOH solid content were prepared by mixing the freeze-dried ChNW powder with PVOH solution. All mixtures were homogenized using an Ultra Turrax mixing at 2000 rpm for 10 minutes and then ultrasonicated for 2 minutes using a 14 mm tip at 50% of the maximum power. The pure PVOH and resulting ChNW-PVOH nanocomposite suspensions were then degassed before casting into a polystyrene Petri dish and dried in an oven at 40 °C for 1 day to obtain the complete dried solid films. Before testing, samples were conditioned at 23 °C and 55% relative humidity in a desiccator with a supersaturated solution of $Mg(NO_3)_2{\cdot}6H_2O$ until a constant weight was reached.

Thermogravimetric analysis (TGA). TGA was carried out using a thermogravimetric analyzer (PerkinElmer model, TGA 4000). Samples of approximately 20 mg were prepared in a ceramic crucible. The samples were heated from 30 °C up to 600 °C at a heating rate of 10 °C min^{-1}, with an N_2 purge of 20 mL min^{-1}.

Tensile test. Tensile testing was performed on dumbbell-shaped specimens according to ASTM D638 and loaded *via* screw action side grips on a tensile micro-tester (Instron 5848), performed at room temperature at the loading rate was set to 5 mm min^{-1}. Testing samples were cut from the dried film using a dog-bone-shaped cutter, having an overall length of 63.5 mm, a gauge length of 9.53 mm, and a width of 3.18 mm. The thickness of the samples was measured using a digital caliper (Mitutoyo, Kawasaki, Japan). At least five samples for each formulation were tested to determine Young's modulus E, the tensile strength, and the strain at break. Young's modulus was calculated from the initial linear region of the stress–strain curves.

3. Results and discussion

3.1 Extraction process and characterization of NADES-ChNW

The detailed process of obtaining NADES-ChNW is described in section 2.2 In brief, chitin powder originating from shrimp shells was first dispersed in NADES (CM) under vigorous overnight stirring at 80 °C. Next, the mixture was injected into the colloidal mill (IKA Magic Lab), filled with aqueous antisolvent in high shear, turbulent conditions, to defibrillate the swollen chitin and liberate the individual crystalline ChNW. The process was followed by centrifugation to remove CM solvent and LMW chitin residues. We first used a combination of scan-

ning and transmission electron microscopy (SEM and TEM) to characterize morphological structures of both the original chitin powder and the NADES-ChNW. Results are shown in Fig. 2.

As shown in the SEM image in Fig. 2(a), the morphology of the original chitin powder particles is highly irregular, with sizes ranging from a few microns to a few hundred microns. Fig. 2(b) shows TEM images of chitin powder dispersed directly in deionized water (without NADES treatment) and applied mechanical treatment in the colloidal mill. This image reveals that the pure mechanical treatment partially defibrillates crystalline particles without releasing individual ChNW. As a result, our observation demonstrates the critical significance of NADES pre-treatment in combination with

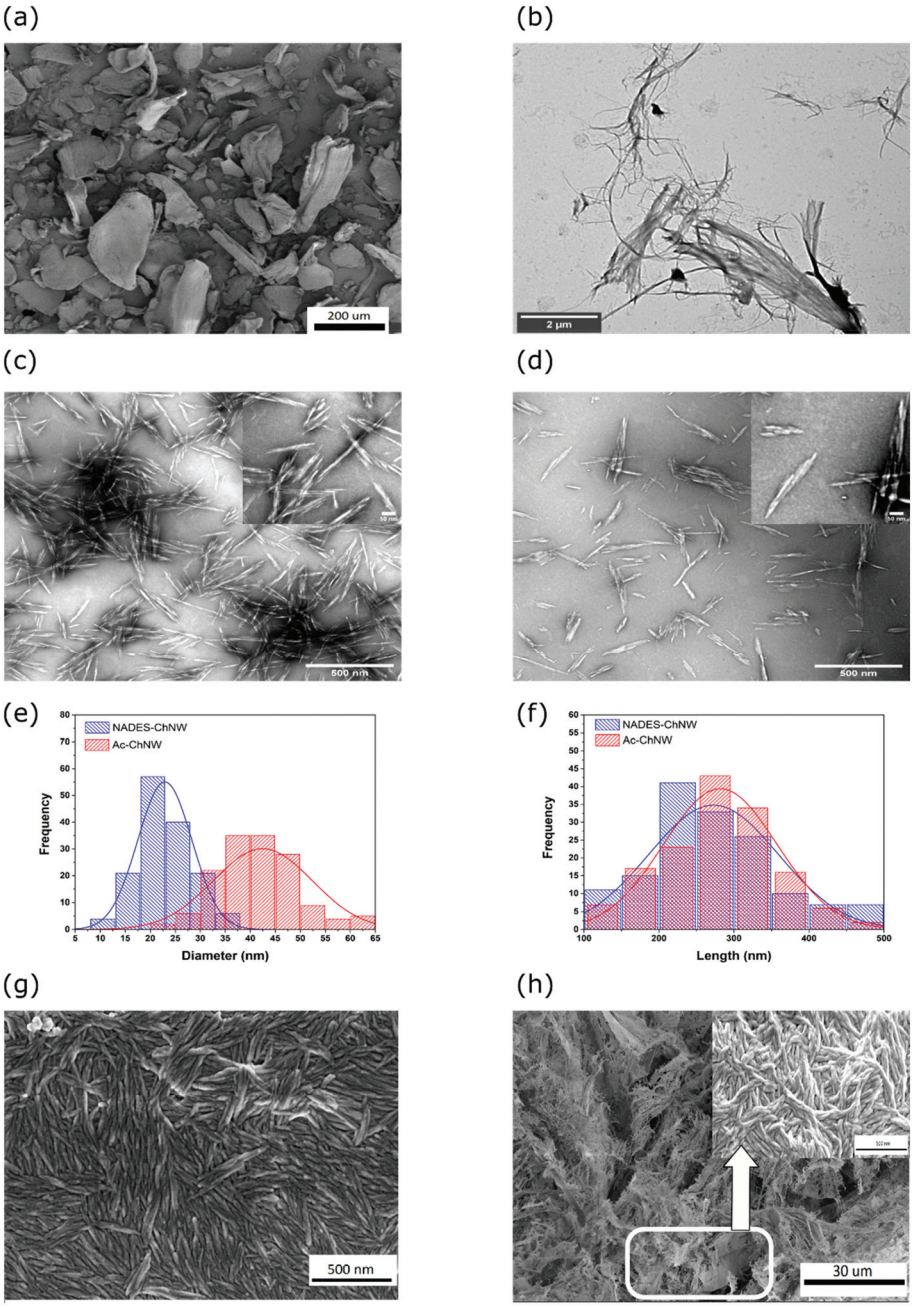

Fig. 2 (a) Scanning Electron Microscope (SEM) images of chitin powder from shrimp shells (scale bar = 200 µm); (b) Transmission Electron Microscope (TEM) images show defibrillation of chitin after mechanical treatment at high shear (15 000 rpm), (scale bar = 2 µm); (c and d) TEM images of a dilute suspension of NADES-ChNW and Ac-ChNW, showing the characteristic needle-like structure. The inlet images in (c and d) show the representative individual nanowhisker (scale bar = 50 nm); (e and f) histograms showing the comparison in diameter and length between NADES-ChNW and Ac-ChNW (g and h) SEM images of fresh NADES-ChNW from aqueous dispersion, and of the powder obtained by freeze-drying the NADES-ChNW dispersions. The insert of (h) shows that individual NADES-ChNW can still be recognized in the freeze-dried powder.

mechanical treatment in the production of chitin nanowhiskers.

TEM images of the chitin nanowhiskers prepared by NADES pre-treatment followed by mechanical treatment and the reference sample prepared by acid hydrolysis are shown in Fig. 2(c and d). An analysis of the dimensions of the NADES-ChNW as obtained from the TEM images is shown in Fig. 2(e and f). We find that the prepared NADES-ChNW have lengths ranging from 100 to 500 nm and widths varying from 15 to 30 nm, respectively. These obtained dimensions of NADES-ChNW were similar to sizes reported in the literature for acid hydrolyzed ChNWs.[17] Meanwhile, the analysis results show that our Ac-ChNW particles have a similar length as NADES-ChNW but a relatively larger width, about 20 to 65 nm. This result could be due to different sources of chitin or the fact that we did not use any further purification of the chitin as obtained from the supplier (Sigma Aldrich). Given the obtained results, we estimated the average aspect ratio (L/d), approximately around 13 for NADES-ChNW and 8 for Ac-ChNW, respectively. The contribution of the amorphous region, as we hypothesize and show in Fig. 1, does not contribute to the actual dimension of nanowhiskers. We argue that it is due to the thickness of this additional layer being of the order of the radius of gyration of a single chitin chain which is relatively small compared to the thickness of the nanowhiskers.

Representative SEM images of the NADES-ChNW are shown in Fig. 2(g). Dispersions of NADES-ChNW were freeze-dried, and the resulting powder was also subject to electron microscopy imaging. As shown in Fig. 2(h), in these freeze-dried powders, the ChNW packs tightly together, but when observed at high magnification (as shown in the inset SEM image), the individual ChNW particles can still be recognized, suggesting that the morphology of the individual nanowhiskers is well-preserved during freeze-drying.

To detect any possible chemical modifications to the chitin due to the NADES extraction, we follow earlier work on Ac-ChNW and use the FT-IR analysis method.[30] The results are shown in Fig. 3, which shows normalized FT-IR spectra for the O–H stretching and carbonyl stretching regions for native chitin powder, NADES-ChNW, Ac-ChNW.

All FT-IR spectra show characteristic absorption peaks of α-chitin, the major component of the chitin powder from shrimp shells. In particular, the absorption peak representing the O–H stretching appeared at 3443 cm^{-1}. The other two absorption bands at 3264 cm^{-1} and 3105 cm^{-1} are assigned to N–H stretching and intramolecular NH bonding. The amide I band split into two absorption peaks at 1656 cm^{-1} and 1620 cm^{-1} are governed by the intramolecular hydrogen bonding between –C═O– and N–H groups. Additionally, the amide II absorption bands derived from C–N–H stretching and N–H bending appeared at 1550 cm^{-1}.

Since we observe no noticeable differences in the FT-IR spectra before and after NADES extraction of ChNW, we concluded that the NADES extraction does not lead to any chemical modifications of the chitin polymers. The obtained Ac-ChNW in this study does not show any significant change in chemical functional group compared to the native chitin. This finding contrasts with what was shown before for acid hydrolysis,[30] where the authors reported that acid extraction leads to partial deacetylation of the native chitin. It is probably attributed to the purification steps at which chitin materials are subjected to a series of chemical treatments. It is noticeable that the peaks for the NADES-ChNW appear to be somewhat sharper. As in previous studies,[17] this can be attributed to the higher purity and possibly higher crystallinity of the chitin in the NADES-ChNW compared to that in the original chitin powder.

Besides the FT-IR, we also employed solid-state ^{13}C NMR to further check for possible chemical modifications of the chitin backbone during the NADES treatment. Chemical shifts are summarized in Table S1.† The ^{13}C CP/MAS NMR analysis signals shown in Fig. S1† again confirm the characteristic of α-chitin, the predominant allotropic form of chitin in shrimp

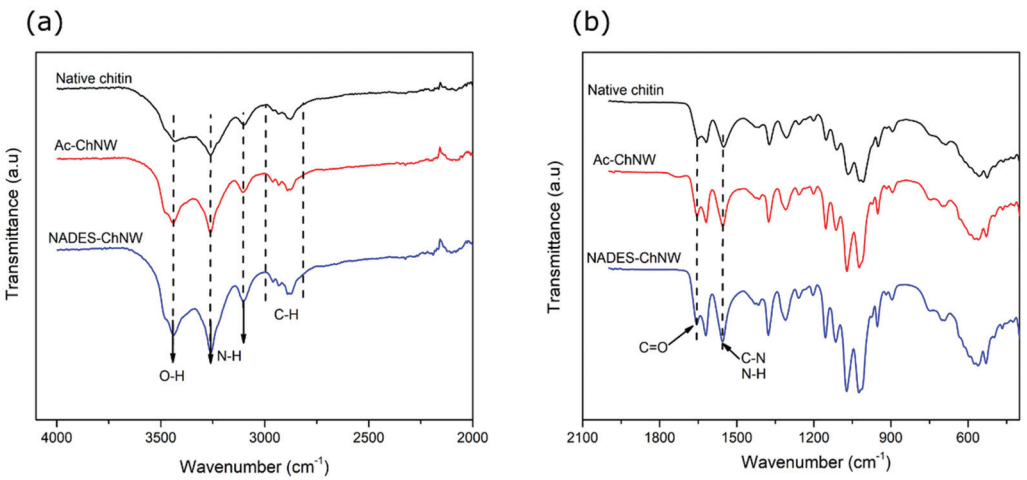

Fig. 3 Comparison between FT-IR spectra of native chitin powder, NADES-ChNW, and Ac-ChNW (a) OH-region (b) carbonyl region.

shells.[33] Furthermore, ^{13}C CP/MAS NMR spectra are identical before and after extraction. The ^{13}C CP/MAS NMR analysis also determines the degree of deacetylation (DA) of the Chitin in the original chitin powder, the freeze-dried NADES-ChNW, and Ac-ChNW. We find a minor increase of DA value after the NADES extraction, from 99.0% for the original chitin powder to 100.2% for the NADES-ChNW. Therefore, we can conclude that there are no indications of significant chemical modifications of the chitin during the NADES extraction. The obtained results are comparable to what has been observed in the case of ChNW obtained *via* acid hydrolysis.[30,34] The corresponding DA value of Ac-ChNW is 104.2%.

To elucidate the degree of crystallinity of the NADES-ChNW, we employed X-Ray Diffraction (XRD). Results are shown in Fig. 4. Spectra for the original chitin powder and the NADES-ChNW are practically identical, with diffraction peaks characteristic for α-chitin at 2θ values of respectively 9.3°, 12.5°, 19.1°, 20.7°, 23.1°, and 26.2°, corresponding to (020), (021), (110), (120), (130), and (013) reflections, respectively. Quantitative analysis of the spectra shows that crystallinity is somewhat higher for the NADES-ChNW (91.5%) than for the original chitin powder (88.8%), which can attribute to partial removal of the low molecular amorphous chitin during the post "washing" process, which is the combination of centrifugation and dialysis (see section 2). The crystallinity index (CrI) for NADES-ChNW is comparable to that of from another recent study on producing ChNW using betaine hydrochloride and ferric chloride hexahydrate.[28] The value of CrI for Ac-ChNW is 97.2%. Indeed, the earlier analysis also found increases in crystallinity upon ChNW isolation.[20] For acid hydrolysis, the increase in crystallinity of the ChNW as determined using the XRD technique is typically attributed to hydrolysis of the amorphous chitin. These data also align with our hypothesis that NADES-ChNW has some residual amorphous chitin, which is basically absent in Ac-ChNW.

To establish whether the chitin can be fully or partially dissolved in the CM NADES, we also used XRD to obtain spectra for chitin powder dispersed in the CM NADES. Results are shown in Fig. 4c, where spectra of the original chitin and the NADES-ChNW are compared with the XRD spectra of dispersion of increasing concentration of chitin powder in CM-NADES. Similar characterization was reported when ionic liquids were attempted to dissolve chitin and chitosan.[35] As can be seen clearly from the inset, for samples with concentrations higher than 3 wt%, we can still recognize the prominent crystalline peak of chitin at 19.1°. Hence, we conclude that the CM-NADES could not dissolve the chitin material completely but swell the amorphous regions in the native chitin. Another study showed that the swelling behavior of α-Chitin is mainly attributed to the disruption of the inter-and intra-molecular hydrogen bonds, and the crystalline state appears to be lost entirely during this swelling.[36] In this respect, the NADES CM showed the effectiveness of disrupting hydrogen bonds in crystalline chitin structure. The full dissolution status might be obtained when prolonging the solubilization process or reducing chitin concentration. Based on these findings, we can predict that in our case, the NADES CM pre-treatment primarily swells the amorphous regions, with some modest disruption of the hydrogen bonds in the crystalline chitin structure, and a small portion of the crystalline chitin structure might also be swollen.

3.2 NADES-ChNW dispersion stability and rheology

We further investigated the colloidal stability properties, including hydrodynamic diameter and zeta potential of NADES-ChNW suspensions, and compared these properties with those of reference Ac-ChNW suspensions. We use Dynamic Light Scattering (DLS) and Electrophoretic Light Scattering (ELS) to determine the effective hydrodynamic diameter and zeta potential as a function of pH and salt concentration for very diluted NADES-ChNW and Ac-ChNW suspensions.

Before discussing our results, we want to point out that one needs to be very careful when interpreting the data from the

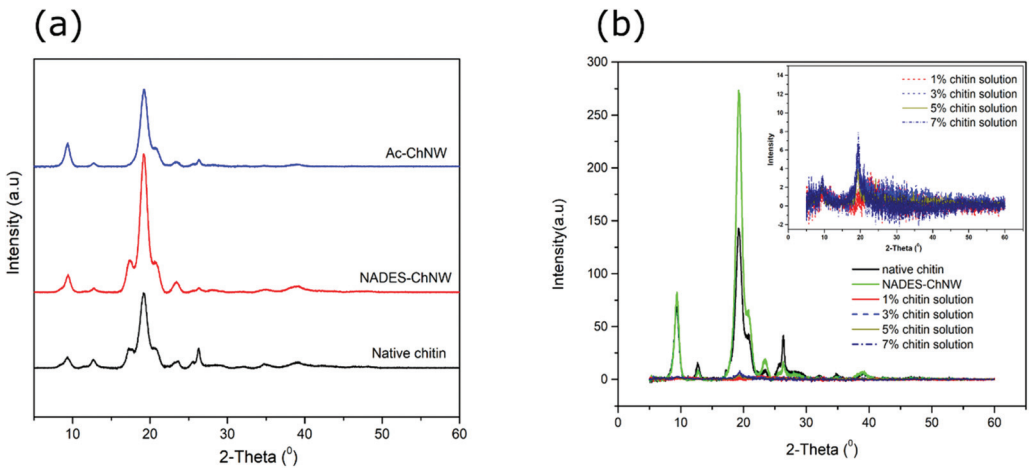

Fig. 4 XRD spectra of (a) native chitin, freeze-dried NADES-ChNW, and Ac-ChNW, and (b) comparison between native chitin, prepared NADES-ChNW, and Chitin in NADES mixture with different concentrations by weight.

effective hydrodynamic diameter with the assumption that the particles are spherical. It is obviously a vast oversimplification for the case of high aspect ratio, rod-like particles where it is known to be incorrect. Therefore, we used the hydrodynamic diameter for qualitative observations of the main trends of colloidal stability as function of pH or electrolyte concentration and as indicators for the destabilization and aggregation of the suspensions.

As illustrated in Fig. 5a and b, highly diluted suspensions of NADES and Ac-ChNW exhibit quite similar stability behavior as a function of pH, with a slightly broader pH stability window for NADES-ChNW (which can be further proven by doing salt titration or studying the behavior of concentrated suspensions at instability onset). These results indicate that both NADES-ChNW and Ac-ChNW have similar surface charges, while the higher pH stability could be attributed to steric stabilization for the case of NADES-ChNW due to the presence of amorphous chitin on their surface (see Fig. 1). To confirm it, we performed salt titration at fixed pH = 4 (see Fig. 5c and d).

As illustrated in Fig. 5d, the zeta potentials of both suspensions are almost identical, indicating a very similar surface charge. However, as shown in Fig. 5c, Ac-ChNW destabilizes more rapidly with increasing ionic strength and forms significantly larger aggregates, as indicated by the effective hydrodynamic diameter. Overall, when comparing at the same conditions (pH and ionic strength), the effective hydrodynamic diameters of Ac-ChNW are consistently larger than those of NADES-ChNW, consistent with TEM size measurements.

In an attempt to confirm the findings from the zeta potential measurements, which indicate that NADES and Ac-ChNW have similar surface charges, we performed the conductometric titration.[32] This method is used to determine the amount of NaOH needed to neutralize the fully protonated, positively charged amino group ($-NH_3^+$) present on the surface of 1 gram of NADES-ChNW or Ac-ChNW. Results are shown in Fig. S2,† showing the ionic conductivity and pH value as a function of the volume of titrant NaOH. From the titration curve, we can estimate an approximate 7.37 mmol NaOH per gram of NADES-ChNW and 1.28 mmol NaOH per gram of Ac-ChNW are needed to neutralize the protonated amino groups on their surface (see ESI†). When comparing with reported data in the literature, we see that the estimated amount of NaOH needed to neutralize the amino groups of Ac-ChNW prepared in this work is higher than that in the literature,[37] which is probably due to the difference in chitin sources or because we performed the acid hydrolysis process without any additional chitin purification steps. If our assumption for the similar surface charge (at same pH and salt concentration) of both ChNW is correct, it would also mean that they must have comparable amino groups density, given these groups are the origin of chitin nanowhiskers surface charge.

Furthermore, given that both whiskers have the same average length, but NADES-ChNW has a twice smaller width (see Fig. 2g and h), they should have roughly twice larger total surface area (see ESI†) than the acid hydrolyzed ones, which in turn would mean that we will need a twice larger amount of NaOH per 1 g of nanowhiskers to neutralize the amino groups NADES-ChNW. However, one can see from the conductometric titration that the measured difference is not 2 times but 6 times larger, which indicates that the surface charge on both types of whiskers is not similar (which is unlikely given how similar are the zeta potentials of these suspensions), or that our assumptions are too crude. Nevertheless, we see qualitative agreement between these two sets of data, which is encouraging.

To summarize, for very diluted suspension, we have observed that NADES and Ac-ChNW have similar colloidal stability as a function of pH and ionic strength, with NADES-ChNW having a slightly larger pH stability window and destabilizes at higher ionic strengths. We hypothesize that the increased stability is not attributable to the surface charge (which, based on the zeta potential measurements, appears to be almost identical) but to the short-range steric stabilization provided by the amorphous region on the surface of NADES-ChNW, which acts as a polymer brush.

To further investigate this effect, we performed experiments with concentrated suspensions at pH = 6, at their electrostatic instability borderline, and where the short-range steric stabilization should be more pronounced. These results are shown in Fig. 6. First, visual observations of dispersions of 5% (w/w) of ChNW are shown in Fig. 6a. While strong aggregation and sedimentation occur quickly for the Ac-ChNW dispersions, there are no visible signs of destabilization for the NADES-ChNW, which looks homogeneous and has a gel-like consistency (indicating the ability to form a self-supporting, elastic network). These observations could explain that Ac-ChNWs form much denser aggregates when destabilized. As a

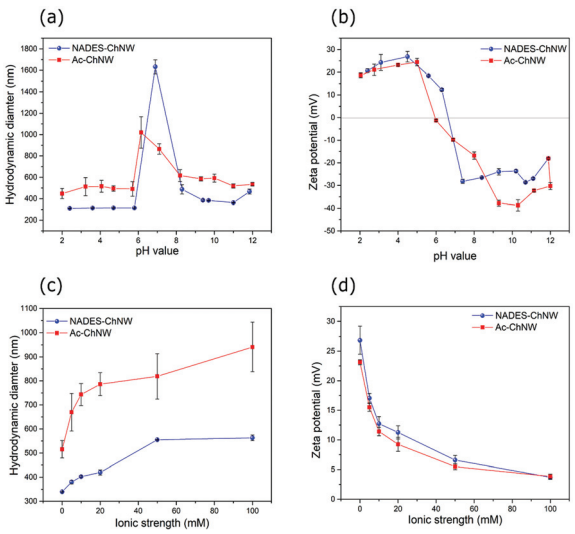

Fig. 5 Effect of pH value (a and b) and ionic strength (c and d) on the colloidal properties, including hydrodynamic diameter and zeta potential of NADES-ChNW and Ac-ChNW. All samples were prepared in an aqueous system with 0.1 wt% ChNW. The pH value of these suspensions was kept at 4 when studying ionic strength's effect.

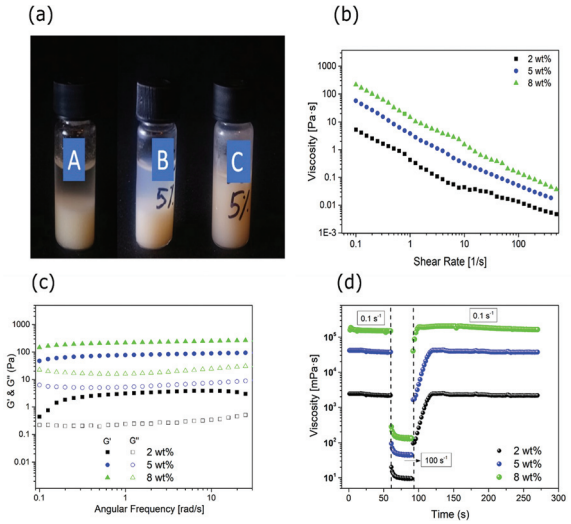

Fig. 6 (a) Aqueous suspension of (A) native chitin powder, (B) 5 wt% Ac-ChNW, and (C) 5 wt% NADES-ChNW. The pH values of these ChNW suspensions are around 6. (b) The shear-rate dependence and (c) frequency dependence; G' (solid points) and G'' (open points); of different aqueous suspensions with various concentrations of freeze-dried NADES-ChNW with different solid concentrations at 2 wt%, 5 wt%, 8 wt%, respectively (d) time-dependent behavior of redispersed NADES-ChNW suspension at different shear-rate conditions: at 0.1 s^{-1}, 100s^{-1} and 0.1 s^{-1}, respectively.

result, they sediments quickly and cannot form a self-supporting network until very large concentrations. Conversely, due to their short-range steric repulsion, NADES-ChNW can form significantly looser and softer aggregates that "percolate" at much lower concentrations and create self-supporting networks, thereby preventing sedimentation and phase separation. To qualitatively illustrate and prove this point, we performed a series of dilution experiments from 5 wt% suspensions starting from pH = 6 and diluting them with pH = 6 buffer. The results are shown in Fig. S4.† From Fig. S4b,† one can see that 2.5 wt% NADES-ChNW suspension at pH = 6 is still stable and homogeneous, suggesting that NADES-ChNW can still form a self-supporting network that prevents phase separation. The phase separation for this system occurs at concentrations below 2 wt%, forming two layers – the top one essentially depleted from ChNW and the bottom layer rich in ChNW. From Fig. S4A,† one can see that Ac-ChNW is unstable in all concentrations. From the ratio between the volume of sediment segment and the total suspension as shown in Fig. 6a, it can be estimated that stable Ac-ChNW suspensions will have a concentration of 10–12.5 wt%. It is consistent with another recent study,[38] where authors studied the rheological behavior of concentrated (20 wt%) suspensions of ChNW obtained using different methods.

Given that all NADES-ChNW suspensions (2–8 wt%) at pH = 6 are stable and homogeneous, we continued investigating their rheological behavior (see Fig. 6b and c). Similar measurements are impossible to be done with Ac-ChNW samples due to phase separation. Not surprisingly, we found that all nanowhiskers suspensions are highly shear-thinning (Fig. 6b) and show weakly elastic behavior with almost no frequency-dependent elastic moduli ranging from 1–100 Pa for concentrations in the range of 2–8 wt%. This observation again confirms the ability of the system to form a self-supporting elastic network, which is highly transient, though as shown in Fig. 6d, with very weak thixotropy and with fast relaxation seen from the fact that the initial zero-shear viscosity is rapidly recovered after a breakdown of the network structure at high shear. Again, we want to emphasize that very diluted suspensions at the same conditions are unstable due to the lack of long-range electrostatic stabilization and are stable at higher concentrations due to the short-range steric stabilization (due to the presence of unhydrolyzed amorphous chitin on their surface).

3.3 NADES-ChNW as fillers in composite films applications

Finally, we investigate how the NADES-ChNW performs as fillers for reinforcing polymer films, a typical application for which ChNW is considered.[13,14] In Fig. 7(a and b), we show representative stress–strain curves of polyvinyl alcohol (PVOH) films reinforced with NADES-ChNW and Ac-ChNW, respectively. We find that the reinforcement effect is much stronger for the NADES-ChNW than for the Ac-ChNW. In addition, we see that a monotonic behavior with increasing NADES-ChNW concentrations, which is not the case for 8% Ac-ChNW, where we see significant deviation (probably due to a very inhomogeneous sample due to much poorer Ac-ChNW dispersibility at this concentration). For values of Young's moduli, tensile strength, and strain at break for all samples, we refer to the ESI, shown in Fig. S6 and Table S2.†

All the nanocomposite samples were found to achieve greater stress values at break than that of the pure PVOH film,

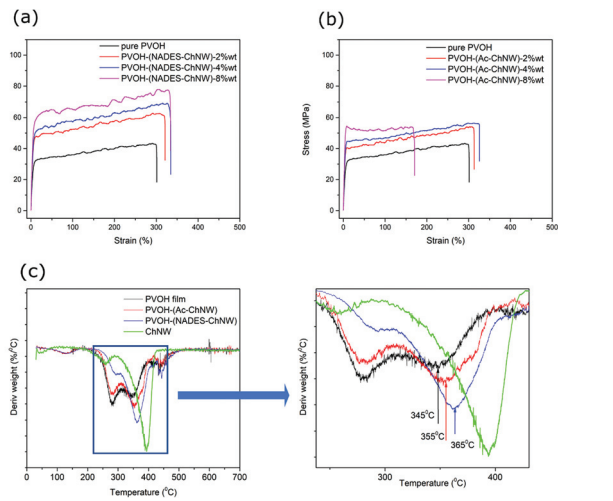

Fig. 7 Stress–strain curves of representative PVOH-ChNW nanocomposite film (a) with NADES-ChNW, PVOH-(NADES-ChNW); (b) with Ac-ChNW, PVOH (Ac-ChNW); (c) derivative thermogravimetric (DTG) curves of ChNW (green), pure PVOH film (black) and PVOH-nanocomposites film with 10 wt% loading of Ac-ChNW (red color), and NADES-ChNW (blue color).

indicating that chitin nanowhiskers would reinforce the PVOH matrix and increase the resistance to plastic deformation. Furthermore, the tensile strength increased with increasing the concentration of chitin nanofiller, and the highest elastic modulus was observed at ChNW-PVOH (8 wt%) nanocomposite samples. There was a slight difference between the elastic modulus values of two sets of PVOH nanocomposites (Ac-ChNW and NADES-ChNW), which is not surprising given that the effect on the elastic modulus is driven by the volume fraction and less sensitive to the aspect ratio. However, the absolute stress values and tensile strength are different, indicating better compatibility between NADES-ChNW and PVOH matrix. These results suggest that incorporating nanoparticles in the polymer matrix would improve the stiffness of PVOH.

To better understand the effect of large amounts (10 wt%) of either Ac-ChNW or NADES-ChNW inclusions on the thermal stability of the composite films, we used Thermogravimetric analysis (TGA). Results are shown in Fig. 7(c). Overall, we find that the pure PVOH films degrade faster than pure ChNW and that the composite films have intermediate behavior. For a more detailed analysis of the TGA results, we refer to the ESI Table S3.† Overall, the main effect that we highlight is that weight loss occurs slower and at higher temperatures for the films with NADES-ChNW compared to those with Ac-ChNW.

The lower reinforcement effect, the more rapid failure observed in the mechanical measurements, and the lower stability observed in TGA suggest that the NADES-ChNW incorporates better with the PVOH film than the Ac-ChNW. We also find support for this picture in the macroscopic appearance of the ChNW containing films (ESI Fig. S5a†), which are much smoother and more homogeneous for the NADES-ChNW composites film. In contrast, for Ac-ChNW composite films, we can observe the visible surface wrinkles and formation of regions with different refractive indexes indicating a heterogeneous distribution of ChNW.

4. Conclusions

In summary, we have developed a novel method producing chitin nanowhiskers by using a specific NADES CM to pre-treat native chitin followed by mild mechanical processing (defibrillation). The use of different types of (NA)DES can be extended, as reported in a previous study.[27] The composition of the (NA)DES components seems to have less impact on the production of ChNW because, with the identical NADES CM, Yuan *et al.* reported the composition of CC : MA (1 : 2), whereas we used CC : MA at 1.5 : 1 molar ratio. However, in this study, we also emphasize the role of mechanical treatment in the production of ChNW. We have shown that both these treatments play a critical role, and using only one of them is not sufficient.

Most importantly, we found that NADES-ChNW has better properties when compared to Ac-ChNW at both high-water activity (dispersion stability, thickening) and low activity (reinforcement of polymer films) applications. We hypothesize that the NADES (mostly) swells the amorphous regions in the native chitin material, which is then disrupted by the high shear to release the individual nanocrystalline regions, which have reminders of chitin from the amorphous regions on their surface. These regions are absent in Ac-ChNW since they are most likely to be hydrolyzed. We have hypothesized that these amorphous chitin remains can act as polymer brushes and provide an additional short-range stearic stability for the ChNW dispersions, which can be seen in the onset of electrostatic destabilization (close to the isoelectric point of chitin or at high salt concentrations).

Contrary to the traditional method of using acid hydrolysis to generate chitin nanowhiskers, we believe that our approach based on the use of NADES based extraction combined with mechanical treatment leads to ChNW with higher functionality and is more energy-efficient, uses less harmful chemicals, and generates less harmful chemicals wastewater than the conventional approach by acid hydrolysis. Practically, after the ChNW production, the DES/NADES solvents can be easily recycled using rotation evaporators or distillation processes, showing the green character of the used solvents and the production route as a whole.[29,39,40] In addition, the NADES extraction leads to higher yields since the NADES extraction can be done at least 7 wt% chitin, whereas acid hydrolysis is typically done at roughly half of this concentration.[14] Additionally, for acid hydrolysis, one typically needs to compromise between good ChNW properties and yield.[16,17]

Our findings also reveal that the NADES-ChNW can be freeze-dried without losing structure or functionality are very encouraging; however, some further work needs to demonstrate full scale-up potential by using an alternative drying process (like spray drying). In addition, the dried NADES-ChNW could be employed as a green rheological modifier to replace inorganic additives in coating applications, particularly as antibacterial coatings or water-based coating systems.[41–43] The shear-thinning behavior and absence of strong thixotropy of the NADES-ChNW suspensions are favorable properties in mixing, handling, and storage.

Finally, we demonstrated that in low water activity applications, such as fillers for reinforcing polymer films, the NADES-ChNW have functional advantages, which we speculate are due to the better interaction of the more hydrophilic NADES-ChNW with the PVOH polymer. In short, the extraction of ChNW using NADES in combination with high mechanical treatment is more sustainable than the conventional acid hydrolysis approach and leads to NADES-ChNW with some additional functional benefits in both high- and low water applications.

Author contributions

All authors contributed equally to writing the manuscript. The experimental research investigation, figures, and visualizations were performed by HVDN. The initial conceptualization and grant application were done by SDS. SDS and RDV acted as

project supervisors and have equally contributed to the interpretation of the experimental results.

Conflicts of interest

There are no conflicts to declare.

Acknowledgements

This work has been financially supported by Unilever Research in The Netherlands and the Graduate School VLAG, The Netherlands. The authors appreciate the assistance provided by Marcel Giesbers for scanning electron microscopy and Rob de Haas for transmission electron microscope imaging.

Notes and references

1 Y. Zhu, C. Romain and C. K. Williams, *Nature*, 2016, **540**, 354–362.
2 S. Tanodekaew, M. Prasitsilp, S. Swasdison, B. Thavornyutikarn, T. Pothsree and R. Pateepasen, *Biomaterials*, 2004, **25**, 1453–1460.
3 F. Shahidi, J. K. V. Arachchi and Y.-J. Jeon, *Trends Food Sci. Technol.*, 1999, **10**, 37–51.
4 S. A. Figueiredo, J. Loureiro and R. Boaventura, *Water Res.*, 2005, **39**, 4142–4152.
5 J. L. Shamshina, P. Berton and R. D. Rogers, *ACS Sustainable Chem. Eng.*, 2019, **7**, 6444–6457.
6 T. Hahn, E. Tafi, A. Paul, R. Salvia, P. Falabella and S. Zibek, *J. Chem. Technol. Biotechnol.*, 2020, **95**, 2775–2795.
7 M. Mincea, A. Negrulescu and V. Ostafe, *Rev. Adv. Mater. Sci.*, 2012, **30**, 225–242.
8 Y. Wu, T. Sasaki, S. Irie and K. Sakurai, *Polymer*, 2008, **49**, 2321–2327.
9 Y. Qin, X. Lu, N. Sun and R. D. Rogers, *Green Chem.*, 2010, **12**, 968–971.
10 L. Heath, L. Zhu and W. Thielemans, *ChemSusChem*, 2013, **6**, 537–544.
11 W.-C. Tsai, S.-T. Wang, K.-L. B. Chang and M.-L. Tsai, *Polymers*, 2019, **11**, 719.
12 M. V. Tzoumaki, D. Karefyllakis, T. Moschakis, C. G. Biliaderis and E. Scholten, *Soft Matter*, 2015, **11**, 6245–6253.
13 A. J. Uddin, M. Fujie, S. Sembo and Y. Gotoh, *Carbohydr. Polym.*, 2012, **87**, 799–805.
14 M. Paillet and A. Dufresne, *Macromolecules*, 2001, **34**, 6527–6530.
15 E. Niinivaara, J. Desmaisons, A. Dufresne, J. Bras and E. D. Cranston, *ACS Appl. Nano Mater.*, 2021, **4**(8), 8015–8025.
16 J.-F. Revol and R. Marchessault, *Int. J. Biol. Macromol.*, 1993, **15**, 329–335.
17 A. G. Pereira, E. C. Muniz and Y.-L. Hsieh, *Carbohydr. Polym.*, 2014, **107**, 158–166.
18 Y. Fan, T. Saito and A. Isogai, *Biomacromolecules*, 2008, **9**, 1919–1923.
19 Y. Fan, T. Saito and A. Isogai, *Biomacromolecules*, 2008, **9**, 192–198.
20 S. Ifuku, M. Nogi, K. Abe, M. Yoshioka, M. Morimoto, H. Saimoto and H. Yano, *Biomacromolecules*, 2009, **10**, 1584–1588.
21 S. Ifuku, K. Yamada, M. Morimoto and H. Saimoto, *J. Nanomater.*, 2012, **2012**, 645624.
22 A. P. Abbott, D. Boothby, G. Capper, D. L. Davies and R. K. Rasheed, *J. Am. Chem. Soc.*, 2004, **126**, 9142–9147.
23 J. A. Sirvio, M. Visanko and H. Liimatainen, *Biomacromolecules*, 2016, **17**, 3025–3032.
24 Y. Liu, B. Guo, Q. Xia, J. Meng, W. Chen, S. Liu, Q. Wang, Y. Liu, J. Li and H. Yu, *ACS Sustainable Chem. Eng.*, 2017, **5**, 7623–7631.
25 Y. Ma, Q. Xia, Y. Liu, W. Chen, S. Liu, Q. Wang, Y. Liu, J. Li and H. Yu, *ACS Omega*, 2019, **4**, 8539–8547.
26 C. Mukesh, D. Mondal, M. Sharma and K. Prasad, *Carbohydr. Polym.*, 2014, **103**, 466–471.
27 Y. Yuan, S. Hong, H. Lian, K. Zhang and H. Liimatainen, *Carbohydr. Polym.*, 2020, 116095.
28 S. Hong, Y. Yuan, K. Zhang, H. Lian and H. Liimatainen, *Nanomaterials*, 2020, **10**, 869.
29 H. V. D. Nguyen, R. De Vries and S. D. Stoyanov, *ACS Sustainable Chem. Eng.*, 2020, **8**, 14166–14178.
30 J. D. Goodrich and W. T. Winter, *Biomacromolecules*, 2007, **8**, 252–257.
31 M. Jaworska, K. Sakurai, P. Gaudon and E. Guibal, *Polym. Int.*, 2003, **52**, 198–205.
32 S. Farris, L. Mora, G. Capretti and L. Piergiovanni, *J. Chem. Educ.*, 2012, **89**, 121–124.
33 G. Cárdenas, G. Cabrera, E. Taboada and S. P. Miranda, *J. Appl. Polym. Sci.*, 2004, **93**, 1876–1885.
34 M. K. Jang, B. G. Kong, Y. I. Jeong, C. H. Lee and J. W. Nah, *J. Polym. Sci., Part A: Polym. Chem.*, 2004, **42**, 3423–3432.
35 H. Xie, S. Zhang and S. Li, *Green Chem.*, 2006, **8**, 630–633.
36 M. Rinaudo, *Prog. Polym. Sci.*, 2006, **31**, 603–632.
37 E. Belamie, P. Davidson and M. Giraud-Guille, *J. Phys. Chem. B*, 2004, **108**, 14991–15000.
38 W. M. Facchinatto, D. M. Dos Santos, A. de Lacerda Bukzem, T. B. Moraes, F. Habitzreuter, E. R. de Azevedo, L. A. Colnago and S. P. Campana-Filho, *Carbohydr. Polym.*, 2021, **273**, 118563.
39 S.-L. Cao, W.-M. Gu, W.-D. Ou-Yang, D.-C. Chen, B.-Y. Yang, L.-H. Lai, Y.-D. Wu, Y.-J. Liu, J. Zhu and W.-J. Chen, *Carbohydr. Polym.*, 2019, **213**, 304–310.
40 S. Hong, Y. Yuan, Q. Yang, P. Zhu and H. Lian, *Carbohydr. Polym.*, 2018, **201**, 211–217.
41 Y. Tan, Y. Liu, W. Chen, Y. Liu, Q. Wang, J. Li and H. Yu, *ACS Sustainable Chem. Eng.*, 2016, **4**, 3766–3772.
42 T. Zhong, M. P. Wolcott, H. Liu and J. Wang, *Carbohydr. Polym.*, 2019, **226**, 115276.
43 H.-L. Nguyen, T. H. Tran, L. T. Hao, H. Jeon, J. M. Koo, G. Shin, D. S. Hwang, S. Y. Hwang, J. Park and D. X. Oh, *Carbohydr. Polym.*, 2021, **271**, 118421.

